

## THERMOELECTRIC GENERATOR HEAT PERFORMANCE STUDY ABOUT IMPROVED FIN STRUCTURES

by

**Tie WANG\* and Shaolei MA**

School of Automobile and Transportation, Shenyang Ligong University, Shenyang, China

Original scientific paper  
<https://doi.org/10.2298/THSCI150801064W>

*This paper involves an exhaust gas waste heat recovery system for vehicles, which uses thermoelectric modules and a heat exchanger to produce electric power. Based on summarizing the latest research of vehicle exhaust thermoelectric generator, it presents two new fin structures for the cylindrical heat exchanger in a thermoelectric generator system. It mainly studies the thermal performance of two kinds of 3-D cylindrical heat exchanger models including spiral-fin heat exchanger with variable pitch in a CFD simulation environment. In terms of interface temperature and thermal uniformity and based on an evaluation method of the temperature uniformity for the heat exchangers, the thermal characteristics of heat exchangers with different pitch angle of the twisted fins, pitch of spiral fin, fin thickness, and fin height are discussed. Two new fin structures are feasible to enhance the heat transfer performance of heat exchanger.*

Key words: *automotive exhaust heat recovery, fin structure, heat exchanger, temperature uniformity, evaluation method*

### Introduction

The efficiency of traditional internal combustion engines is about 30%, while nearly 40% of the fossil energy is wasted directly through the exhaust or coolant [1]. This paper involves some heat exchangers. A heat exchanger is a heattransfer device used for transfer of internal thermal energy between two or more fluids available at different temperatures [2]. The thermal performance of the heat recovery systems using heat pipe heat exchanger is dependent on the effectiveness of the heat pipe heat exchanger which in turn depends on input heat transfer rate, the evaporator length, working fluid, and its filling ratio [3]. There are thermoelectric modules on the wall of heat exchangers. Electric voltage generates induced by temperature difference across the thermoelectric module (Seebeck effect) [4]. In a 1.5 L car engine under test, 315 W(e) was recovered from the exhaust energy using thermoelectrics under motorway driving (130 km/h), and for a 3 L engine this would increase to around 600 W(e) [5].

According to the advantages and benefits of thermoelectric generator (TEG) system, many studies on it are proposed. A hexagonal cross-section hot box was used with aluminum radiator-based cold plates used as a heat dissipater [6]. Parametric evaluations are considered to assess the influence of heat exchanger, geometry (including Hexagonal and cylindrical configurations), and thermoelectric module configurations to achieve optimization of the baseline model [7]. The power generator assembled with 96 TEG modules had an installed power of 500 W at a temperature difference of around 200 °C [8]. He *et al.* [9] investigated the impacts

\* Corresponding author, e-mail: wangtiesylg@126.com

of the number and the coverage rate on the heat exchanger of the TEG which is used to extract heat from an automotive exhaust pipe and turns the heat into electricity *via* simulations. A multi objective optimization based on artificial neural network and genetic algorithm are applied on the obtained results from numerical outcomes for a finned-tube heat exchanger in diesel exhaust heat recovery [10].

In terms of interface temperature and thermal uniformity, the thermal characteristics of heat exchangers with different internal structures are discussed. The maze shape has slightly higher interface temperature at the front end, but lowers at the outlet. However, the fish-bone design shows better uniformity [11].

### Simulation on liquid-solid conjugate heat transfer of heat exchangers with different fins structures and evaluation method of wall temperature

#### Simulation model of the heat exchangers

In this paper, the exhaust TEG system shown in fig. 1 generally includes heat exchanger, cooling unit, thermoelectric modules, and clamping and fixed device. It is concluded

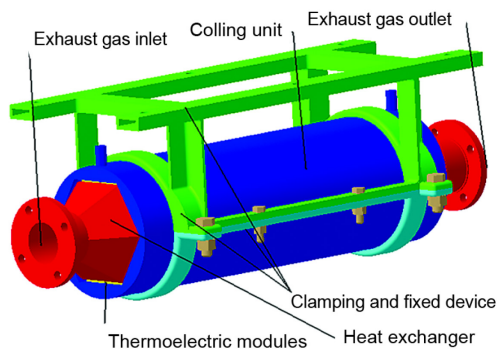


Figure 1. The TEG system

structure, the heat exchanger and thermoelectric modules are placed in hollow space. Exhaust gas flows into the heat exchanger to provide a heat source. The cooling water is pumped into the water tank to form the cold side. Then, electric power is generated due to the temperature difference between the two sides of the modules based on the Seebeck effect [11].

We propose two kinds of cylindrical heat exchangers: twisted-fin heat exchanger, and spiral-fin heat exchanger. The heat exchanger with twisted fins which is called twisted-fin heat exchanger is a hexagonal-prism-shaped aluminum box, whose channel is cylindrical, fitting averagely twelve fins on the radial, as shown in fig. 2. The fin can enhance dramatically the effect of heat transfer and is a twisted aluminum plate at a certain height and thickness whose structural shape is like the teeth of cylindrical helical gear. The diameters of the intake and exhaust manifolds of the heat exchanger are both 0.06 m. The inner diameter of cylindrical channel is 0.134 m, and the total length of the heat exchanger is 0.8 m. This paper mainly studies the thermal performance of the heat exchangers. For twisted-fin heat exchanger, the heat exchangers which have different twistedly finned pitch angle (0, 5, 10, 15, and 20 degrees), fin thickness (0.001, 0.002, 0.003, 0.004, and 0.005 m), and fin height (0.035, 0.040, 0.045, 0.050, and 0.055 m) are built.

that the layout with the front three-way catalytic converter has an advantage over the other layout mode under current conditions [12]. Thermoelectric modules containing a large number of n-type and p-type semiconductors, arranged in couples, are clamped with sufficient compressive force between a heat exchanger connected to the exhaust pipe and cooling water tank in an exhaust-based TEG like a sandwich by clamping and fixed device. There are inner fins inside of the cylindrical heat exchanger with hot exhaust gases flowing around them. The cooling unit is a cylinder with hexagonal hollow

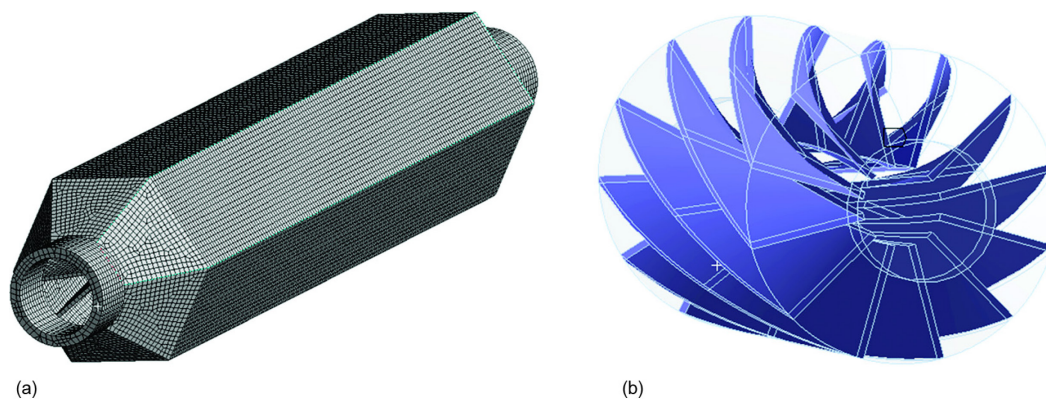


Figure 2. (a) Finite element model with grid, (b) fin structure of twisted-fin heat exchanger

Compared with twisted-fin heat exchanger, the heat exchanger with spiral fin which is called spiral-fin heat exchanger has the same external dimensions, but its internal fin is spiral, as is shown in fig. 3. For spiral-fin heat exchanger, the heat exchangers which have different spirally finned pitch (0.015, 0.030, 0.045, 0.060, and 0.075 m), fin thickness (0.001, 0.002, 0.003, 0.004, and 0.005 m), and fin height (0.030, 0.035, 0.040, 0.045, and 0.050 m) are built.

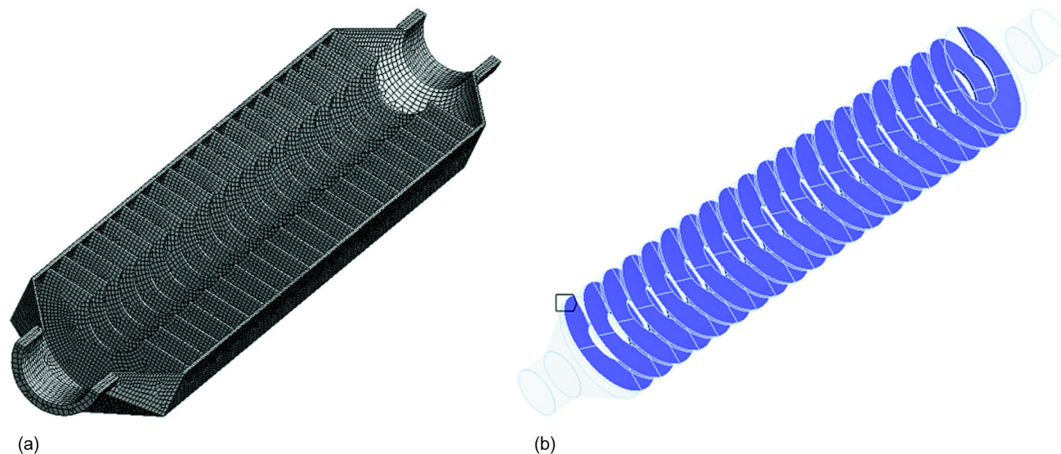


Figure 3. (a) Half sections of finite element model with grid, (b) fin structure of spiral-fin heat exchanger

### ***Boundary conditions of the simulation models***

To get the parameters about boundary conditions of the simulation models, this paper builds a 1-D engine model in a GT-Power simulation environment. It is built on the basis of a 4-cylinder 2.0 L gasoline engine [13]. The simulation results show, at engine speed of 4000 rpm, the TEG inlet velocity is 54 m/s and the inlet temperature is 797 K. The CFD was used to simulate the exhaust gas-flow within the heat exchanger, enabling simulation of the interface temperature distribution [11]. This paper uses CFD code CFX to carry out the solution.

### Boundary conditions of the inlet and outlet of the heat exchangers

The TEG inlet is set as the velocity entrance, the inlet velocity is 54 m/s and the temperature of the exhaust gas is 797 K. The TEG outlet is set as a pressure export, and the outlet pressure is the ambient static pressure, so that the back pressure at the exit can be set to 0 [14].

### Boundary conditions of solid domain and gas domain

Liquid-solid conjugate heat transfer simulation is mainly the coupling of a solid domain and a gas domain about heat transfer. The standard  $k-\varepsilon$  turbulence model is adopted in the CFD simulation of the heat exchanger, assuming that the flow is fully turbulent. In light of TEG inlet temperature (797 K), the physical parameters of the exhaust gas can reference parameters of the exhaust gas at 773 K, which is shown in tab. 1. Additionally, convective heat transfer coefficient is a parameter related to material performance, the surrounding air temperature, fluid velocity

**Table 1. Physical parameters of the exhaust gas [15]**

	$\rho$ [kgm <sup>-3</sup> ]	$\lambda$ [Wm <sup>-1</sup> K <sup>-1</sup> ]	$c_p$ [Jkg <sup>-1</sup> K <sup>-1</sup> ]	$\mu$ [kgm <sup>-1</sup> s <sup>-1</sup> ]
Exhaust flow (773 K)	0.457	0.0656	1185	$3.48 \cdot 10^{-5}$

and many other conditions, and this paper focuses on qualitatively analyzing what influence the fin size has on the heat exchange performance. So, the coefficient of convective heat transfer between the outer surface of the exchanger and the air is set to 30 W/m<sup>2</sup>K, assuming that the environment temperature is 300 K. The boundary conditions of the other heat exchangers are set as the same.

### Evaluation method of the wall temperature uniformity for heat exchanger

One-sixth of outside wall is considered according to the symmetry of the heat exchanger. Primarily, create rectangular regions, where the semiconductor thermoelectric modules are placed, in the same hot surface (the red rectangular area) of heat exchanger simulation models. As shown in fig. 4, there are twenty-six thermoelectric modules in total in the red rectangular area, with two rows and thirteen columns. Position number is the column number from left to right.

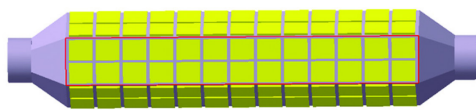


**Figure 4. Rectangular regions in an outside surface of heat exchanger**

Referencing the temperature uniformity coefficient of flat-plate heat exchanger [16], this paper gets an evaluation indicator of the outside wall temperature uniformity for the cylindrical heat exchanger: temperature uniformity coefficient  $\gamma$ .

$$\gamma = 1 - \frac{1}{n^{1/\varepsilon}} \sum_{i=1}^n \frac{|T_i - T_{\text{mean}}|}{T_{\text{mean}}} \quad (1)$$

where for hexagonal-prism-shaped heat exchanger,  $\varepsilon = 6$ . The  $\varepsilon$  value can not only revise errors that all surface areas of heat exchanger are not taken into account during the evaluation, but also increase the gap between temperature uniformity values.

The temperature coefficient  $\gamma$  varies from 0 to 1. If  $\gamma = 1$ , it means the outside wall temperature of heat exchanger is the same everywhere [16].

### Simulation results and discussion

In terms of interface temperature and thermal uniformity, the thermal characteristics of heat exchangers with different pitch angle of the twisted fins, pitch of spiral fin, fin thickness and fin height are discussed.

#### Interface temperature distribution on the twisted-fin heat exchangers and the spiral-fin heat exchangers with different fin thickness

To study the effect of fin thickness on wall temperature of twisted-fin heat exchanger, let twistedly finned pitch angle and fin height be  $10^\circ$  and 0.050 m. The wall temperature variation of the twisted-fin heat exchangers with different fin thickness is measured on basis of the obtained 70 temperature data on the red rectangular surface in fig. 4, as shown in fig. 5(a). According to the simulation results, for twisted-fin heat exchanger, the wall temperature increases with the increase of fin thickness. The schematic of temperature uniformity coefficient  $\gamma$ , backpressure of heat exchanger  $\Delta P$  (the pressure difference between the inlet and the outlet of heat exchanger), and average temperature of hot surface  $T_{\text{mean}}$  with the variation of fin thickness is shown in fig. 5(b). It shows that, with the increase of fin thickness,  $\gamma$  reduces initially then increases,  $\Delta P$  reduces initially then increases and  $T_{\text{mean}}$  increases at a constant in twistedly finned pitch angle and fin height. Taken together, twisted fins of 0.003 m in thickness are more suitable than the other ones for twisted-fin heat exchanger.

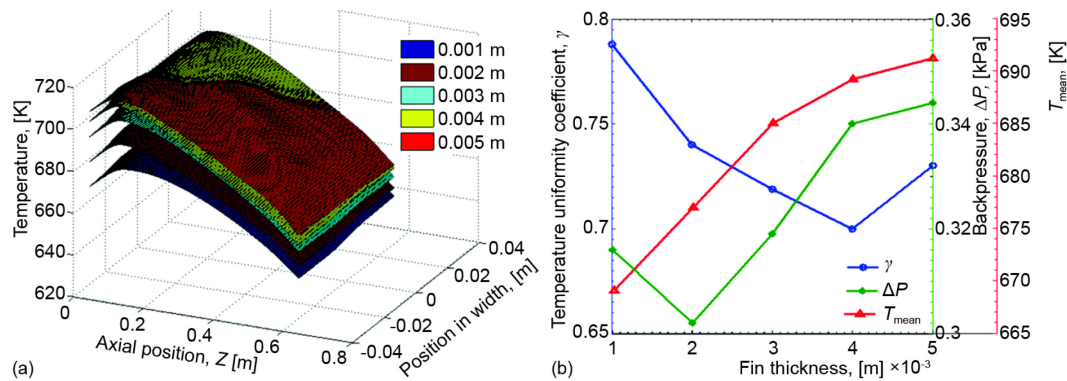
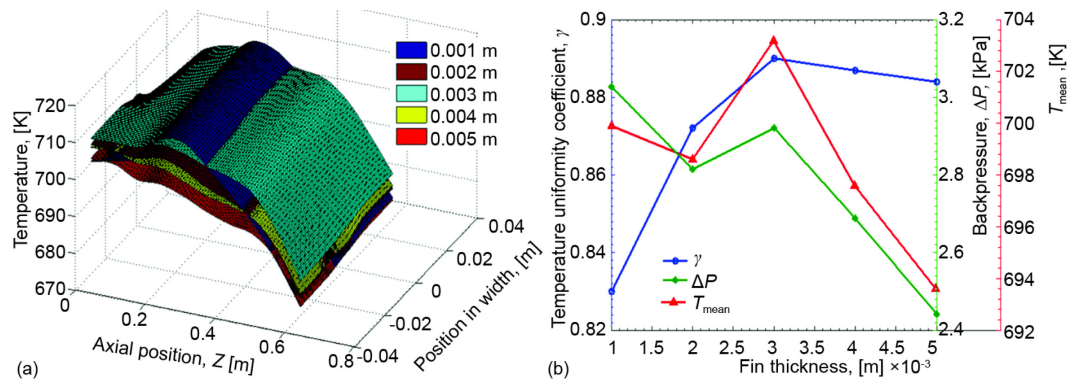


Figure 5. (a) Wall temperature variation of the twisted-fin heat exchangers with different fin thickness, (b) the effect of different fin thickness on some parameters of twisted-fin heat exchanger (for color image see journal web site)

Similarly, for spiral-fin heat exchanger, let pitch of the spiral fin and fin height is 0.030 m and 0.040 m. The wall temperature variation of the spiral-fin heat exchangers with different fin thickness is shown in fig. 6(a). It shows that, for spiral-fin heat exchanger, roughly, the wall temperature increases initially then reduces with the increase of fin thickness. The schematic of  $\gamma$ ,  $\Delta P$ , and  $T_{\text{mean}}$  with the variation of fin thickness is shown in fig. 6(b). It shows that, with the increase of fin thickness,  $\gamma$  increases initially then reduces slightly,  $\Delta P$  reduces roughly, and  $T_{\text{mean}}$  increases initially then reduces generally at a constant in pitch angle of the

twisted fins and fin height. Taken together, spiral fin of 0.003 m in thickness is more suitable than the other ones for spiral-fin heat exchanger.



**Figure 6. (a) Wall temperature variation of the spiral-fin heat exchangers with different fin thickness, (b) the effect of different fin thickness on some parameters of spiral-fin heat exchanger (for color image see journal web site)**

#### *Interface temperature distribution on the twisted-fin heat exchangers with different twistedly finned pitch angle and the spiral-fin heat exchangers with different spirally finned pitch*

To further study the effect of twistedly finned pitch angle on wall temperature of twisted-fin heat exchanger and the effect of spirally finned pitch on wall temperature of spiral-fin heat exchanger, let fin thickness be 0.003 m for both heat exchangers, let fin height be 0.040 m and 0.050 m for twisted-fin heat exchanger and spiral-fin heat exchanger, respectively.

The wall temperature variation of the twisted-fin heat exchangers with different twistedly finned pitch angle is shown in fig. 7(a). It shows that, for twisted-fin heat exchanger, the wall temperature change with the increase of twistedly finned pitch angle is not quite obvious, but the wall temperature is a little higher than that of the heat exchanger without twistedly finned pitch angle. The schematic of  $\gamma$ ,  $\Delta P$ , and  $T_{\text{mean}}$  with the variation of twistedly finned pitch angle is shown in fig. 7(b). It shows that, with the increase of twistedly finned pitch angle,  $\gamma$  reduces initially then increases,  $\Delta P$  increases initially then reduces then increases sharply again, and  $T_{\text{mean}}$  increases initially then reduces at a constant in fin thickness and fin height. Taken together, twisted fins of 15° in pitch angle are more suitable than the other ones for twisted-fin heat exchanger.

Similarly, the wall temperature variation of the spiral-fin heat exchangers with different spirally finned pitch is shown in fig. 8(a). It shows that, for spiral-fin heat exchanger, the wall temperature reduces with the increase of spirally finned pitch. The schematic of  $\gamma$ ,  $\Delta P$ , and  $T_{\text{mean}}$  with the variation of spirally finned pitch is shown in fig. 8(b). It shows that, with the increase of spirally finned pitch,  $\gamma$  increases initially then reduces sharply, both  $\Delta P$  and  $T_{\text{mean}}$  decrease dramatically at a constant in fin thickness and fin height. In addition, the flow speed of the exhaust gas in the internal cavity of the heat exchanger is not too fast or too slow to affect the engine power [14]. Based on simulation results for flow distribution of the spiral-fin heat exchangers with 0.015 m and 0.030 m in spirally finned pitch, the latter is more suitable than the other ones for spiral-fin heat exchanger.

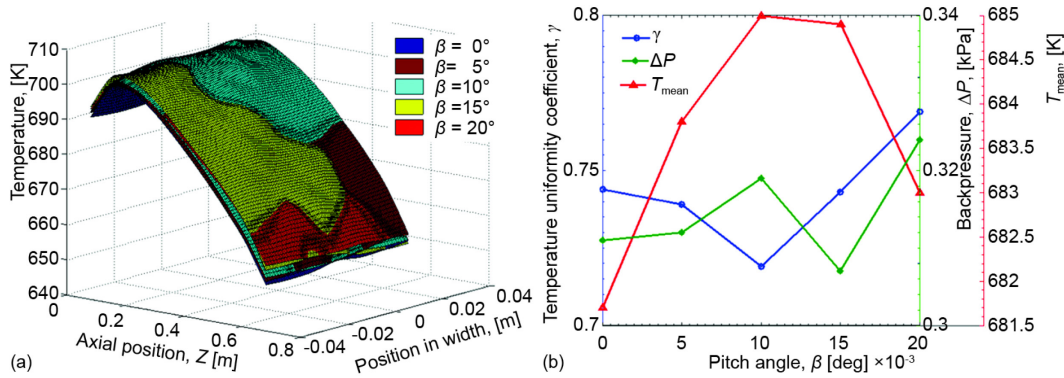


Figure 7. (a) Wall temperature variation of the twisted-fin heat exchangers with different twistedly finned pitch angle,  $\beta$ , (b) the effect of different twistedly finned pitch angle,  $\beta$ , on some parameters of twisted-fin heat exchanger (for color image see journal web site)

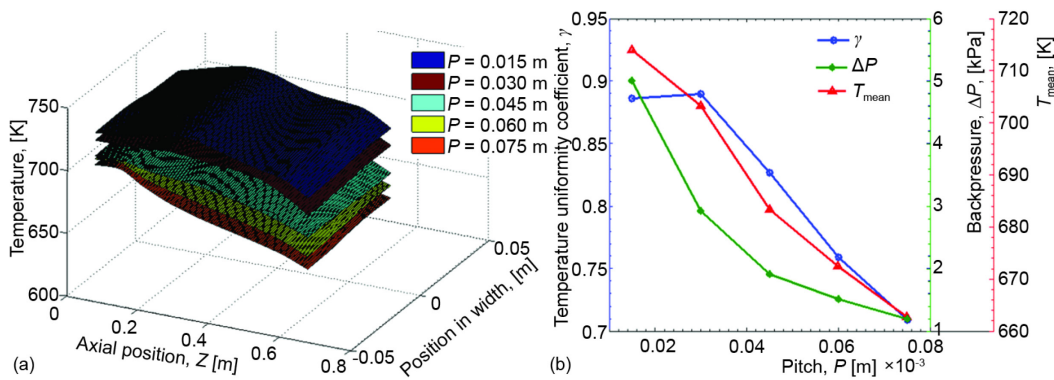


Figure 8. (a) Wall temperature variation of the spiral-fin heat exchangers with different spirally finned pitch,  $P$ , (b) the effect of different spirally finned pitch,  $P$ , on some parameters of spiral-fin heat exchanger (for color image see journal web site)

*Interface temperature distribution on the twisted-fin heat exchangers and the spiral-fin heat exchangers with different fin height*

To go on study, let thickness and finned pitch angle of twisted fins be 0.003 m and 15 deg, while let thickness and finned pitch of spiral fin be 0.003 m and 0.030 m.

The wall temperature variation of the twisted-fin heat exchangers with different fin height is shown in fig. 9(a). It shows that, for twisted-fin heat exchanger, the wall temperature increases with the increase of fin height. The schematic of  $\gamma$ ,  $\Delta P$ , and  $T_{\text{mean}}$  with the variation of fin height is shown in fig. 9(b). It shows that, with the increase of fin height,  $\gamma$  reduces initially then increases then decreases sharply,  $\Delta P$  increases initially then decreases gradually then increases rapidly, and  $T_{\text{mean}}$  increases dramatically at a constant in fin thickness and twistedly finned pitch angle. In light of higher wall temperature, twisted fins of 0.050 m in height are more suitable for twisted-fin heat exchanger.

Similarly, the wall temperature variation of the spiral-fin heat exchangers with different fin height is shown in fig. 10(a). It shows that, for spiral-fin heat exchanger, the wall

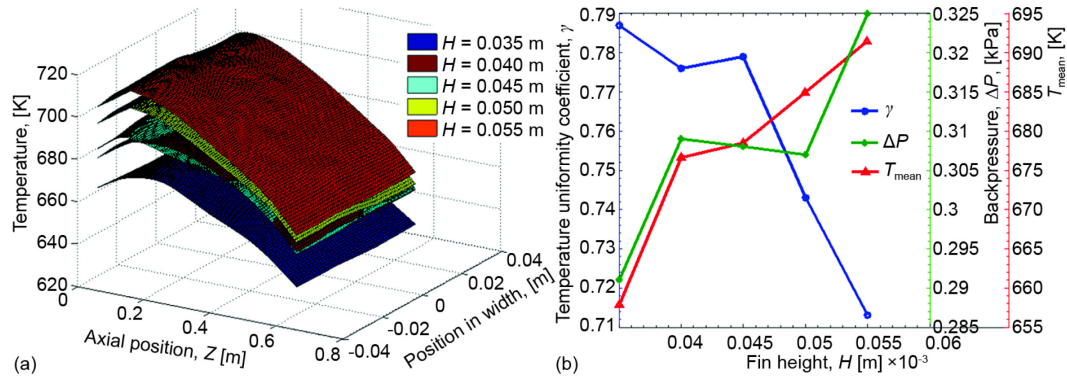


**Figure 9. (a) Wall temperature variation of the twisted-fin heat exchangers with different fin height,  $H$ , (b) the effect of different fin height,  $H$ , on some parameters of twisted-fin heat exchanger (for color image see journal web site)**

temperature increases with the increase of fin height. The schematic of  $\gamma$ ,  $\Delta P$ , and  $T_{\text{mean}}$  with the variation of fin height is shown in fig. 10(b). It shows that, with the increase of fin height,  $\gamma$  increases initially then reduces, both  $\Delta P$  and  $T_{\text{mean}}$  increase dramatically at a constant in fin thickness and spirally finned pitch. Taken together, spiral fin of 0.040 m in height is more suitable for spiral-fin heat exchanger.

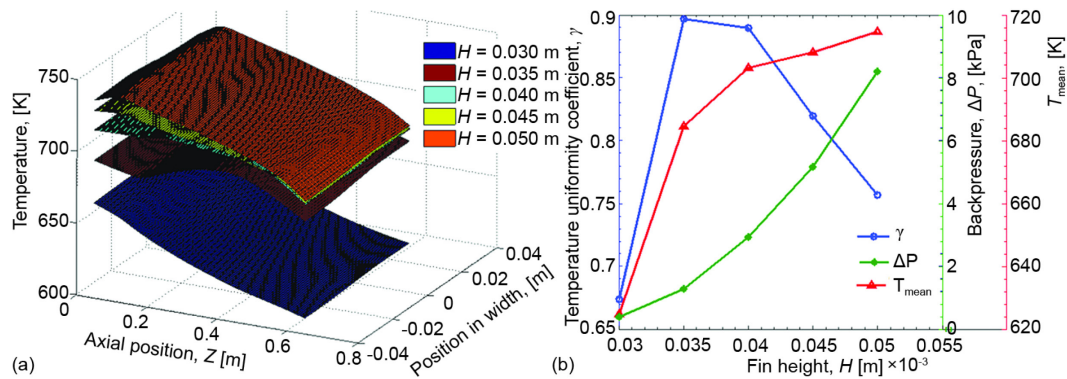


**Figure 10. (a) Wall temperature variation of the spiral-fin heat exchangers with different fin height,  $H$ , (b) the effect of different fin height,  $H$ , on some parameters of spiral-fin heat exchanger (for color image see journal web site)**

Based on the previous simulation analysis, for twisted-fin heat exchanger, the heat exchanger with twisted fins of 0.003 m in thickness, 15° in pitch angle and 0.050 m in height has the better thermal performance. Simulation results for temperature distribution, pressure distribution and flow distribution of the twisted-fin heat exchanger are shown in fig. 11. It shows that the overall temperature appears as a bamboo-shape distribution, the longitudinal temperature gradually reduces. For spiral-fin heat exchanger, the heat exchanger with spiral fin of 0.003 m in thickness, 0.030 m in pitch and 0.040 m in height has the better thermal performance. Backpressure of spiral-fin heat exchanger is higher than that of twisted-fin heat exchanger. But thermal uniformity of spiral-fin heat exchanger is better than that of



twisted-fin heat exchanger. The simulation results details about temperature distribution, pressure distribution and flow distribution of the spiral-fin heat exchanger are discussed later.

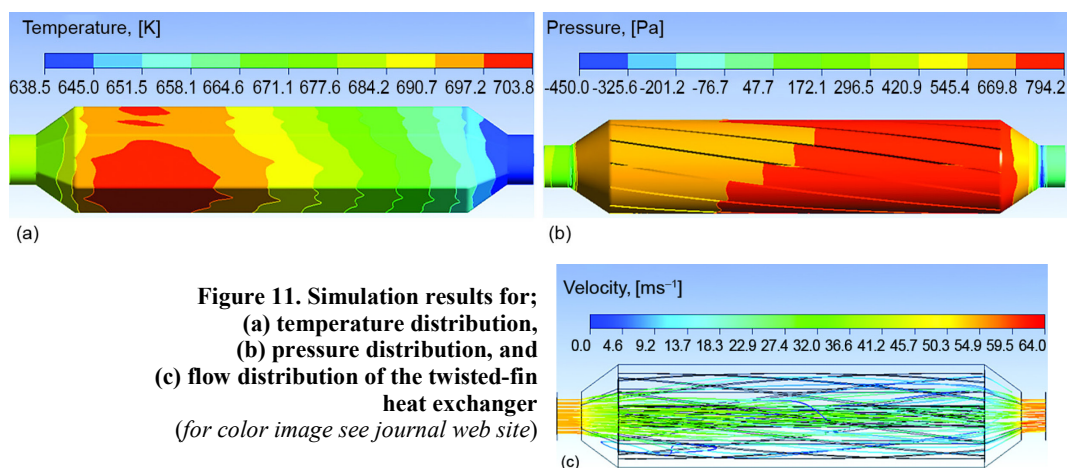


**Figure 11. Simulation results for;**  
**(a) temperature distribution,**  
**(b) pressure distribution, and**  
**(c) flow distribution of the twisted-fin**  
**heat exchanger**  
*(for color image see journal web site)*

### ***Simulation on spiral-fin heat exchanger with variable pitch***

According to the previous simulation results, pitch of spiral fin has a great influence on wall temperature of heat exchanger. The longer pitch is, the higher wall temperature is; otherwise the lower wall temperature is. Based on the spiral fin of 0.003 m in thickness, 0.030 m in pitch and 0.040 m in height, a spiral fin with variable pitch, is built, whose pitch becomes short gradually from exhaust gas inlet to exhaust gas outlet in the range of 0.023 to 0.033 m, as it is shown in fig. 12.

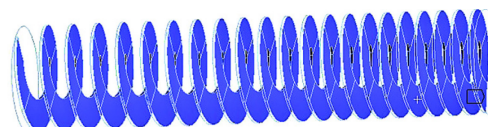


**Figure 12. Fin structure of spiral-fin heat exchanger with variable pitch**

The boundary conditions of the spiral-fin heat exchanger with variable pitch are set as the same as previously. Simulation results for temperature distribution of the old spiral-fin heat exchanger and spiral-fin heat exchanger with variable pitch are shown in fig. 13. For the old spiral-fin heat exchanger,  $T_{\text{mean}}$  is 703.2 K,  $\gamma$  is 0.890. While, for spiral-fin heat exchanger with variable pitch,  $T_{\text{mean}}$  is 702.1 K and  $\gamma$  is 0.965, increasing by 8.4% than the original. As it can be seen from fig. 13, both the longitudinal and transverse temperature distributions are more uniform, the high temperature zone of the heat exchanger expands a lot along the axis and becomes larger.

Simulation results for pressure distribution of the old spiral-fin heat exchanger and spiral-fin heat exchanger with variable pitch are shown in fig. 14. It shows the relative pressure close to the inlet is high and the pressure close to the outlet is small. For the old spiral-fin heat exchanger,  $\Delta P$  is 2.92 kPa. For spiral-fin heat exchanger with variable pitch,  $\Delta P$  is 3.14 kPa, which is more than that of the former. While considering that the backpressure of the automobile exhaust gas is usually 30-40 kPa [14], the pressure distribution is relatively uniform and the backpressure of heat exchanger is acceptable.

Simulation results for flow distribution of the old spiral-fin heat exchanger and spiral-fin heat exchanger with variable pitch are shown in fig. 15. It can be seen that, the gas

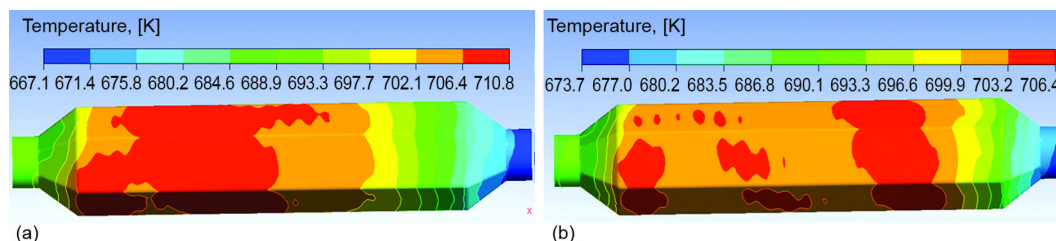


Figure 13. Simulation results for temperature distribution of; (a) the old spiral-fin heat exchanger, (b) spiral-fin heat exchanger with variable pitch (for color image see journal web site)

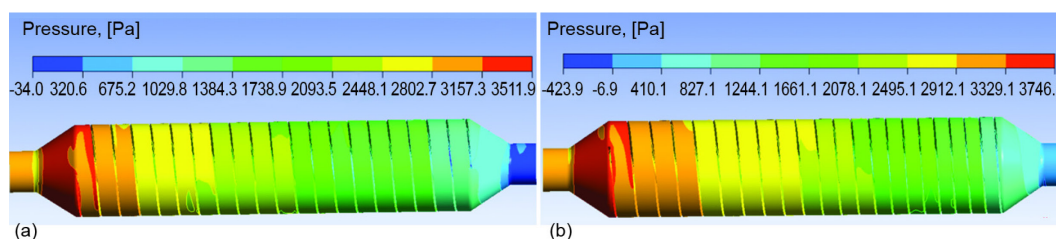


Figure 14. Simulation results for pressure distribution of; (a) the old spiral-fin heat exchanger, (b) spiral-fin heat exchanger with variable pitch (for color image see journal web site)

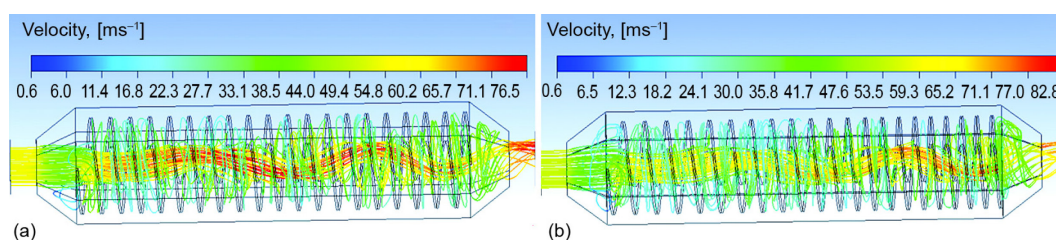


Figure 15. Simulation results for flow distribution of; (a) the old spiral-fin heat exchanger, (b) spiral-fin heat exchanger with variable pitch (for color image see journal web site)

flow moves forward in a spiral, quickly and some of that moves close to the spiral fin. The flow distribution is relatively uniform. The exhaust gas speed in the internal cavity of spiral-fin heat exchanger with variable pitch is a little higher than that of the old spiral-fin heat exchanger.

#### Estimate of the error about simulation results

One-sixth of all surface areas of heat exchanger are taken into account during the evaluation of  $\gamma$ , but the change trend of wall temperature of heat exchanger in exhaust gas flow direction is the same for each face of heat exchanger. So, the evaluation of  $\gamma$  is within the margin. Besides, set residual target  $10^{-6}$ , use full-hexahedral grid in finite element analysis of heat exchanger models and the smallest number of nodes and cells is about 460000 and 580000. In a word, the error of simulation results is within the margin.

#### Conclusions

According to the simulation analysis, the results for two heat exchangers are as follows.

- For twisted-fin heat exchanger, the interface temperature increases with the increase of fin thickness, temperature uniformity reduces initially then increases a little. The interface

temperature change with the increase of pitch angle is not quite obvious, but the interface temperature is a little higher than that of the heat exchanger without twistedly finned pitch angle, temperature uniformity reduces initially then increases. The interface temperature increases with the increase of fin height, temperature uniformity reduces initially then increases then decreases sharply.

- For spiral-fin heat exchanger, the interface temperature increases initially then reduces with the increase of fin thickness, temperature uniformity increases initially then reduces slightly. The interface temperature reduces with the increase of spirally finned pitch, temperature uniformity increases initially then reduces sharply. The interface temperature increases with the increase of fin height, temperature uniformity increases initially then reduces.
- Spiral-fin heat exchanger has the better thermal performance than twisted-fin heat exchanger, but the backpressure of spiral-fin heat exchanger is a lot bigger than that of twisted-fin heat exchanger.
- Spiral-fin heat exchanger with variable pitch has the better thermal performance than the old spiral-fin heat exchanger, but the backpressure of spiral-fin heat exchanger with variable pitch is a little bigger than that of the old spiral-fin heat exchanger.

Twisted fins of 0.003 m in thickness, 15° in pitch angle and 0.050 m in height are better for twisted-fin heat exchanger. Spiral fin of 0.003 m in thickness and 0.030 m in pitch and 0.040 m in height is better for spiral-fin heat exchanger. For heat exchanger, both fin structures are feasible.

### Nomenclature

$c_p$	– air specific heat, [ $\text{Jkg}^{-1}\text{K}^{-1}$ ]
$H$	– fin height, [m]
$n$	– the number of thermoelectric module
$P$	– spirally finned pitch, [m]
$\Delta P$	– backpressure of heat exchanger, [kPa]
$T_i$	– average temperature of $i^{\text{th}}$ rectangular region, [K]
$T_{\text{mean}}$	– average temperature of hot surface, [K]

### Greek symbols

$\beta$	– twistedly finned pitch angle, [degree]
$\gamma$	– temperature uniformity coefficient, eq. (1)
$\varepsilon$	– the number of hot surface
$\lambda$	– thermal conductivity, [ $\text{Wm}^{-1}\text{K}^{-1}$ ]
$\mu$	– dynamic viscosity, [ $\text{kgm}^{-1}\text{s}^{-1}$ ]
$\rho$	– density, [ $\text{kgm}^{-3}$ ]

### References

- [1] Kim, S., et al., A Thermoelectric Generator Using Engine Coolant for Light-Duty Internal Combustion Engine-Powered Vehicles, *Journal of Electronic Materials*, 40 (2011), 5, pp. 812-816
- [2] Liu, Y., et al., Experimental Research on Heat Transfer in a Coupled Heat Exchanger, *Thermal Science*, 17 (2013), 5, pp. 1437-1441
- [3] Mandapati, M. J. K., et al., Thermodynamic Performance Evaluation of an Air-Air Heat Pipe Heat Exchanger, *Thermal Science*, 18 (2014), 4, pp. 1343-1353
- [4] Sippawit, N., et al., A Study of Sensing Heat Flow through Thermal Walls by Using Thermoelectric Module, *Thermal Science*, 19 (2015), 5, pp. 1497-1505
- [5] Rowe, D. M., et al., Weight Penalty Incurred in Thermoelectric Recovery of Automobile Exhaust Heat, *Journal of Electronic Materials*, 40 (2011), 5, pp. 784-788
- [6] Saqr, K. M., et al., Thermal Design of Automobile Exhaust Based Thermoelectric Generators: Objectives and Challenges, *International Journal of Automotive Technology*, 9 (2008), 2, pp. 155-160
- [7] Kumar, S., et al., Thermoelectric Generators for Automotive Waste Heat Recovery Systems, Part II: Parametric Evaluation and Topological Studies, *Journal of Electronic Materials*, 42 (2013), 6, pp. 944-955
- [8] Liu, C. W., et al., A 500 W Low-Temperature Thermoelectric Generator: Design and Experimental Study, *International Journal of Hydrogen Energy*, 39 (2014), 28, pp. 15497-15505

- [9] He, W., *et al.*, Recent Development and Application of Thermoelectric Generator and Cooler, *Applied Energy*, 143 (2015), 1, pp. 1-25
- [10] Hatami, M., *et al.*, Experimental and Numerical Analysis of the Optimized Finned-Tube Heat Exchanger for OM314 Diesel Exhaust Exergy Recovery, *Energy Conversion and Management*, 97 (2015), June, pp. 26-41
- [11] Deng, Y. D., *et al.*, Thermal Optimization of the Heat Exchanger in an Automotive Exhaust-Based Thermoelectric Generator, *Journal of Electronic Materials*, 42 (2013), 7, pp. 1634-1640
- [12] Su, C. Q., *et al.*, Effect of the Sequence of the Thermoelectric Generator and the Three-Way Catalytic Converter on Exhaust Gas Conversion Efficiency, *Journal of Electronic Materials*, 42 (2013), 7, pp. 1877-1881
- [13] \*\*\* Gamma Technologies Inc., GT-SUITE Engine Performance Tutorials, <http://www.doc88.com/p-3137131683727.html>
- [14] Liu, X., *et al.*, Experiments and Simulations on a Heat Exchanger of an Automotive Exhaust Thermoelectric Generation System under Coupling Conditions, *Journal of Electronic Materials*, 43 (2014), 6, pp. 2218-2223
- [15] Zhou, M. F., *et al.*, A Heat Transfer Numerical Model for Thermoelectric Generator with Cylindrical Shell and Straight Fins under Steady-State Conditions, *Applied Thermal Engineering*, 68 (2014), 1-2, pp. 80-91
- [16] Tang, Z. B., *et al.*, Fluid Analysis and Improved Structure of an ATEG Heat Exchanger Based on Computational Fluid Dynamics, *Journal of Electronic Materials*, 44 (2015), 6, pp. 1554-1561